

Quantum sensitivity analysis: a general framework for controlling quantum fluctuations

Shiekh Zia Uddin^{1,2,†}, Nicholas Rivera^{1,3,†}, Devin Seyler², Yannick Salamin^{1,2}, Jamison Sloan², Charles Roques-Carmes^{2,4}, Shutao Xu⁵, Michelle Y. Sander^{5,6,7}, and Marin Soljačić^{1,2}

[†] *These authors contributed equally. E-mail: nrivera@fas.harvard.edu, suddin@mit.edu*

¹ *Department of Physics, Massachusetts Institute of Technology, Cambridge, MA 02139, USA.*

² *Research Laboratory of Electronics, Massachusetts Institute of Technology, Cambridge, MA 02139, USA.*

³ *Department of Physics, Harvard University, Cambridge, MA 02138, USA.*

⁴ *E. L. Ginzton Laboratory, Stanford University, Stanford, California 94305, USA.*

⁵ *Department of Electrical and Computer Engineering and BU Photonics Center, Boston University, Boston, MA 02215, USA.*

⁶ *Division of Materials Science and Engineering, Boston University, Brookline, MA 02446, USA.*

⁷ *Department of Biomedical Engineering, Boston University, Boston, MA 02215, USA.*

Nonlinear systems are important in many areas of modern science and technology. For example, nonlinearity plays an essential role in generating quantum mechanical states of both light and matter. As a result, there has been great interest in understanding the fundamental quantum nature of a variety of nonlinear effects. At the same time, there is currently a large gap between the classical and quantum understanding of nonlinear systems, with the classical understanding being far more developed. To close this gap, we introduce a general new theory which allows us to predict quantum effects in any nonlinear system purely in terms of its classical description. We demonstrate the predictions of our theory in experiments probing quantum fluctuations of intense femtosecond pulses propagating in an optical fiber undergoing soliton-fission supercontinuum generation, a process where broadband radiation is produced by a narrow-band input. Famously, this process is known to be highly noise-sensitive, leading to noisy outputs even from inputs with only quantum fluctuations. In contrast, our experiments uncovered a variety of previously hidden low-noise and noise-robust states arising from quantum correlations and entanglement, in agreement with the predictions of our theory. We also show how the theory points to new design concepts for controlling quantum noise in optics and beyond. We expect that our results will provide a template for discovering quantum effects in a wide variety of complex nonlinear systems.

In the physical world, nonlinear systems offer an enormous range of rich and complex effects, many with wide-ranging implications in fundamental science and technology. The vast majority of the work on nonlinear systems is based on their description according to the laws of classical physics. At the same time, it has become increasingly important to understand the fundamental description of nonlinear systems according to the laws of quantum mechanics.

In part, this is because nonlinear dynamics leads to useful transformations of quantum fluctuations, the fundamental randomness of system states imposed by Heisenberg's uncertainty principle. For example, nonlinearity generically enables generating states with non-classical fluctuation properties, such as squeezed states and entangled states [1], which may enable overcoming noise-related limits on a wide variety of important systems (e.g., interferometers [2, 3], imaging systems [4, 5], communication systems [6, 7], light sources such as lasers and frequency combs [8–11], clocks [12–14], magnetometers [15], and emerging sensors [16, 17]). Historically, the interplay between classical nonlinearity and quantum noise was first experimentally explored in the field of nonlinear optics [18–20]. While this interplay is actively explored in optics, it is now important in a much wider variety of physical platforms including optomechanics [21], spins [22], phonons [23–25], excitons [26], and Josephson junctions [27].

As a result of these successes, there is great interest in developing the fundamental quantum description of ever more complex nonlinear effects. Despite this, the classical understanding of nonlinear systems remains far more advanced than the quantum understanding. This is especially relevant in systems where the classical (mean-field) description involves

strong interactions between many distinct modes or degrees of freedom. In this highly multimode regime, many basic insights into quantum noise are still absent.

Here, we address this knowledge gap with a new theory of quantum fluctuations in nonlinear systems. The theory enables us to understand quantum fluctuations in any nonlinear system purely in terms of the underlying classical description, by analyzing the response of the classical nonlinear system to certain changes in the initial conditions: in other words, by sensitivity analysis. This “quantum sensitivity analysis” provides many new explicit, closed-form guidelines for controlling noise in a wide variety of systems. We demonstrate the predictions of our theory in the context of ultrafast nonlinear optics, through experiments probing quantum noise in a long-studied phenomenon called soliton-fission supercontinuum generation. While this phenomenon is long-known to be a strongly noisy and noise-sensitive process, guided by our theory we experimentally uncover several hidden low-noise and noise-robust states in this phenomenon. We find that these low-noise states originate from the strong quantum correlations that build up during the process of supercontinuum generation. We conclude by discussing some additional predictions of our theory which reveal important concepts for realizing new types of low-noise sources and quantum states in optics and other fields.

I. QUANTUM SENSITIVITY ANALYSIS

We summarize the essential results of our theory of quantum noise in nonlinear systems. Detailed derivations, as well

as additional examples, are shown in the Supplementary Information (SI). Consider a general nonlinear physical system, which can have both electromagnetic field and matter degrees of freedom (see Fig. 1a). Electromagnetic degrees can refer to any type of solution to Maxwell's equation: plane waves modes, cavity modes, temporal modes, etc. Matter degrees of freedom are also broadly defined: these can include a two-level transition in a gain medium, phonons in a fiber or waveguide, or even electrons (see SI for an example with gain). Defining the collection of independent degrees of freedom (and their conjugates) as α, α^* , we define the classical theory of the system as an input-output relation, relating the degrees of freedom at the final time ($\alpha_{\text{out}}, \alpha_{\text{out}}^*$) to those at the initial time ($\alpha_{\text{in}}, \alpha_{\text{in}}^*$). In particular, we write:

$$\alpha_{\text{out}} = F(\alpha_{\text{in}}, \alpha_{\text{in}}^*), \quad (1)$$

where F is some arbitrary function of the light and matter variables (see SI for examples of F).

Now, consider an arbitrary observable X (e.g., intensity, phase, quadrature, position, momentum). From Eq. (1), X is a function of the initial conditions: $X_{\text{out}} = X(\alpha_{\text{in}}, \alpha_{\text{in}}^*)$. In the SI, we show that the quantum noise in X_{out} can be determined in terms of derivatives of the classical input-output relation of Eq. (1), with respect to classical initial conditions: $\partial X_{\text{out}}/\partial \alpha_{\text{in}}, \partial X_{\text{out}}/\partial \alpha_{\text{in}}^*$. In particular, while the mean value of X is governed by the classical dynamics for some fixed initial conditions, the variance, $(\Delta X_{\text{out}})^2$ is given by:

$$\begin{aligned} (\Delta X_{\text{out}})^2 &= v^T C v, \text{ where} \\ v &= \left(\frac{\partial X_{\text{out}}}{\partial \alpha_{\text{in}}} \frac{\partial X_{\text{out}}}{\partial \alpha_{\text{in}}^*} \right)^T \\ C &= \begin{pmatrix} \langle \delta a \delta a \rangle_{\text{in}} & \langle \delta a \delta a^\dagger \rangle_{\text{in}} \\ \langle \delta a^\dagger \delta a \rangle_{\text{in}} & \langle \delta a^\dagger \delta a^\dagger \rangle_{\text{in}} \end{pmatrix}, \end{aligned} \quad (2)$$

where in the correlation matrix C , the operators $\delta a \equiv a - \langle a \rangle, \delta a^\dagger \equiv a^\dagger - \langle a \rangle^*$ refer to the noise creation and annihilation operators of the system modes and $\langle \delta a \delta a \rangle_{ij} = \langle \delta a_i \delta a_j \rangle$ (with similar definitions for the other expectation values). The “in” subscript denotes that the correlation matrix is set by the statistics of the initial state, which allows for straightforward inclusion of the effects of excess noise (thermal or technical), multimode correlations (e.g., entanglement), and phase-sensitive correlations (e.g., from injecting squeezed states into the system at time zero).

This rule, we call the *quantum mechanical law of total variance*, because it essentially prescribes a “quadrature-addition” rule for quantum noise – in parallel to the law of total variance in classical statistics, which shows that the variance of a sum of independent random variables adds in quadrature. Here, we find the same rule for quantum noise, where the relevant noises are the coefficients of C and they are weighted by the “sensitivities”: $\partial X_{\text{out}}/\partial \alpha_{\text{in}}, \partial X_{\text{out}}/\partial \alpha_{\text{in}}^*$, since we are considering in general a nonlinear function of the quantum random variables. The quadrature-addition is especially clear in the simple but important case in which the initial fluctuations of all modes only have uncorrelated vacuum noise (meaning each mode is in a coherent state). In that case:

$$(\Delta X_{\text{out}})^2 = \|\partial X_{\text{out}}/\partial \alpha_{\text{in}}\|^2, \quad (3)$$

and the quantum noise is *entirely* prescribed by the derivatives of the classical problem.

The power of this framework is in the fact that understanding classical dynamics and quantum noise are no longer different problems: one can take existing classical theories and analyze how observables change due to small changes in complex-valued initial conditions. This type of analysis, classically, is referred to as sensitivity analysis [28]. Since here, the shifts are due to quantum fluctuations of different degrees of freedom, we use the name quantum sensitivity analysis. This type of analysis also shows which degrees of freedom affect the outputs the most, since their noise effects all add in quadrature. Eq. (2) also gives a powerful analytical decomposition of quantum noise into two components: initial correlations (C , which is quantum), and sensitivities (the derivatives, which are classical). The quantum noise contributions in any nonlinear system can thus now be referred to in a unified way. Moreover, the connection to sensitivity analysis enables computationally *efficient* numerical computation of quantum noise: namely, the sensitivities in Eq. (2) can be calculated by numerical adjoint methods (e.g., [29–32]), which enables calculating the noise in an observable much faster than black-box quantum noise numerical methods based on stochastic differential equations or linearization techniques [100] [1, 33, 34]. We employ such adjoint-based calculations in what follows (Fig. 2). All together, these various advantages allowed us to analyze quantum noise in many new settings, developing new analytical insights in both experiments and theory.

Before moving on to examples, we mention that the input-output theory need not be expressible in terms of complex wave amplitudes: it could also be specified for example by a collection of positions and momenta (in the case of particles), or angular momenta (in the case of spins), or combinations of different types of degrees of freedom. The case of positions and momenta is developed in the SI and considered in Fig. 5.

A. Example: the quantum theory of optical limiting

To give the reader a flavor for our theory, we give a pedagogical example of quantum sensitivity analysis using a simple example in nonlinear optics involving two modes. The result here also applies to more general nonlinear wave systems. From this, we will be able to build a new closed-form quantum mechanical theory of a classically well-known nonlinear optics effect called optical limiting. Optical limiting is a phenomenon in which large changes in the intensity of light at the input of some system lead to small changes in the output. This concept had been explored for generating quantum states of light whose intensity fluctuations are below the shot-noise level associated with quantum-mechanical coherent states (coherent states are the “most classical” states of the quantized electromagnetic field, and are produced by ideal lasers) [35, 36]. For inputs at the shot-noise level, the photon-number variance is equal to the mean. States with intensity noise below the shot-noise level are called sub-Poissonian or intensity-squeezed states [37].

An example of an optical limiting system that produces sub-

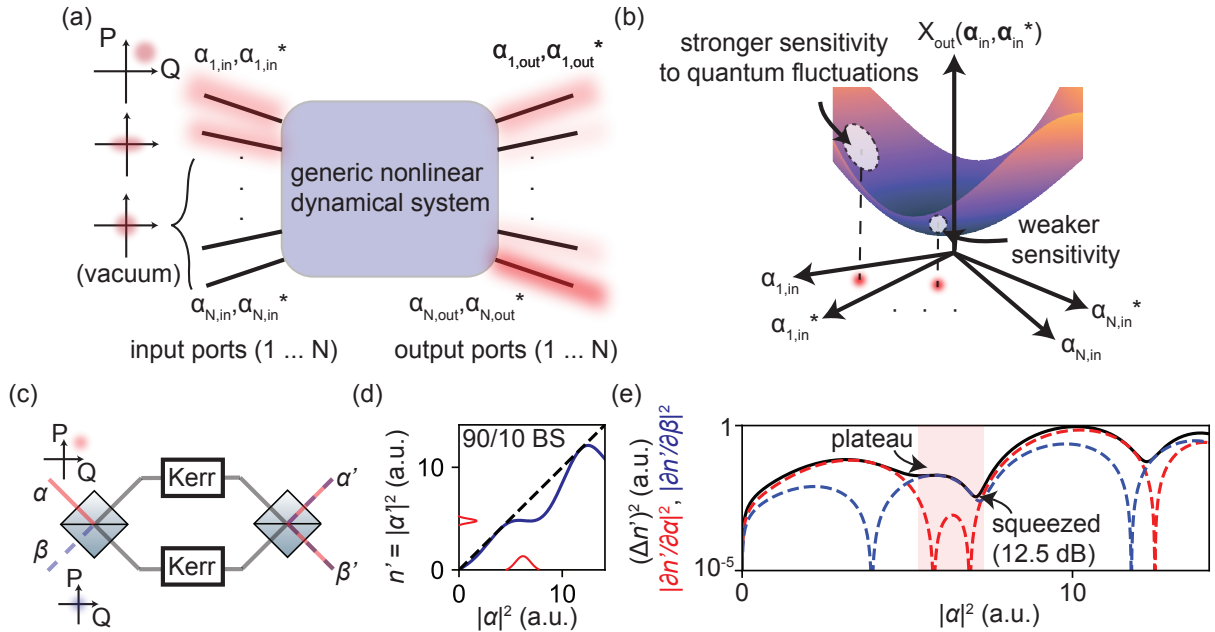


FIG. 1: **Quantum sensitivity analysis and the quantum theory of optical limiting.** (a) A generic nonlinear dynamical system can be specified as a map that connects inputs and outputs. These inputs can be complex wave amplitudes, particle positions and momenta, spins, etc. The inputs can be populated with excitations, or can be ‘dark’, indicating vacuum states for wave systems. The inputs undergo linear and nonlinear interactions represented by the purple box. These inputs have quantum fluctuations, schematically illustrated as phase-space distributions, though our theory also captures the effect of correlations between these inputs. (b) The crux of the framework is to analyze the sensitivity of observables $X\{\alpha, \alpha^*\}$ to vacuum level shifts (quantum fluctuations) in the inputs $\alpha(0), \alpha^*(0)$. Larger (smaller) gradients translate to larger (smaller) noise in X . (c-e) Example of quantum sensitivity analysis in nonlinear optics. (c) A nonlinear Mach-Zehnder interferometer composed of two beamsplitters with equal splitting ratios, and two arms with identical length and nonlinear index. (d) Output number of photons (blue) in the α' port as a function of α , assuming the input to have a constant-intensity envelope. The axes are scaled so that $|\alpha|^2$ corresponds to the nonlinear phase accrued by the input. The transmission features a plateau where, classically, variations in the intensity (shown in red) would be mapped to much weaker variations of the output. (e) Variance of the output photon number as a function of input. Red and blue curves show the contributions of the bright (α) and dark (β) ports to the overall noise. At the point of greatest intensity-noise reduction (12.5 dB squeezing), the noise comes entirely from the dark port.

Poissonian light is shown in Fig. 1c. It is a nonlinear Mach-Zehnder interferometer (MZI) consisting of one beamsplitter, followed with two arms of propagation of equal length, and a second beamsplitter identical to the first. The two arms of propagation contain Kerr nonlinear media, such that the light propagating in these arms undergoes a phase shift ϕ proportional to the intensity of light in each arm. Quantitatively: $\phi \sim \theta|\alpha|^2$, where θ is the strength of the nonlinearity and $|\alpha|^2$ is the number of photons in the beam [101]. Assuming the amplitude reflection/transmission coefficient of the splitters is r/t , the output field in the α' port is (see SI):

$$\alpha' = -re^{i\theta|\alpha|^2}(-r\alpha + it\beta) + ite^{i\theta|\alpha|^2}(it\alpha - r\beta). \quad (4)$$

In what follows, we will consider the case where the splitting ratio is 90/10, as this leads to optimal squeezing or noise reduction [35, 36]. The transmission of the system into the α' port is shown in Fig. 1d: it features a plateau over some range of powers (or nonlinear phase shifts). This is an optical limiting point, as classically, input intensity variations (indicated in red) map to smaller output intensity variations. The resulting intensity noise into the α' port ($n' = |\alpha'|^2$) is shown in

Fig. 1e: it has a minimum in the plateau as expected. Its noise is about 12.5 dB below the shot-noise level.

Traditionally, works observing this effect attributed the minimum to the optical limiting effect: the incident intensity noise (shot noise) goes through a region with flat input-output, and so its noise is reduced. Even then, it was known that this explanation is not correct, as it predicts zero fluctuations (ignoring the higher-derivative contributions, which are very small), and it predicts zero fluctuations for any splitting ratio. Not only are the fluctuations not zero, but for ratios closer to 50/50 (e.g., 60/40), the classical optical limiting points lead to noise above the shot-noise level [38]. Surprisingly, despite substantial work on this interferometer, there was no quantitative understanding of why 12.5 dB was the maximum for 90/10, and also how to go beyond this number, even theoretically. It was similarly unclear why 60/40 fails to provide squeezing at the optical limiting point [39]. With quantum sensitivity analysis we will now (a) explain why 12.5 dB is the minimum and (b) show how to go beyond this number. In the SI, we also explain from quantum sensitivity analysis why 60/40 doesn’t provide squeezing.

Quantum sensitivity analysis states that the intensity noise

in the output is given in terms of the derivatives of the classical input-output relation of Eq. (4), as:

$$(\Delta n')^2 = \left| \frac{\partial n'}{\partial \alpha} \right|^2 + \left| \frac{\partial n'}{\partial \beta} \right|^2 = n \left(\frac{\partial n'}{\partial n} \right)^2 + \left| \frac{\partial n'}{\partial \beta} \right|^2. \quad (5)$$

The contributions from the α and β ports are shown in Fig. 1e. Focus on the plateau region, shaded in red: the contribution from the α port is negligible. This is the classical optical limiting intuition. The overall noise is limited by the sensitivity of this particular interferometer to inputs in the dark port. Thus, to go beyond this, we need to minimize the classical sensitivity of the interferometer to variations in the dark port amplitude, while maintaining a small slope of the intensity input-output curve. In Sec. III, we show how to do this. Before moving on, we also note that quantum sensitivity analysis can go beyond the two-mode case, making predictions of how quantum noise transforms when femtosecond pulses propagate through these nonlinear MZIs. We experimentally probed this case, revealing several intriguing effects which our theory can explain (see Sec. IV. D and Figs. 8-10 of the SI).

II. PROBING THE QUANTUM OPTICAL NATURE OF SUPERCONTINUUM GENERATION

In this section, we experimentally test the predictions of our theory. We performed experiments on a long-studied classical nonlinear optics platform, finding new effects: high-power femtosecond pulses propagating through a single-mode optical fiber. In particular, we developed high-resolution probes of the quantum noise and correlations associated with the phenomenon of supercontinuum generation, a process in which a narrow-band input pulse becomes much broader in frequency. Using these probes, in conjunction with our theory, we identified a series of very low-noise and noise-robust states that go against the standard picture of supercontinuum as a noise-sensitive effect. The origin of many of these low-noise states is quantum correlation (entanglement) that builds up during the process, as well as a remarkable broadband insensitivity of certain wavelengths to vacuum fluctuations.

We start by giving background on the system and the core classical and quantum aspects relevant to our experiments. Classically, a femtosecond pulse propagating in a single-mode optical fiber is subject to dispersion, as well as nonlinearity. The nonlinearity has two main components: an instantaneous component, coming from electronic response of the fiber material (here, silica), and a delayed component, coming from localized vibrational modes (phonons) associated with amorphous silica. The complete classical description is given by an equation of motion for the electric field envelope of the pulse $A(z, t)$ as a function of propagation distance z along the fiber and time t (time defined in the co-propagating frame with the pulse). That equation is called the generalized nonlinear Schrödinger equation, and in the frame moving at the group

velocity of the pulse, is given by [40, 41]:

$$\begin{aligned} \partial_z A(z, t) = i \sum_{k=2}^{\infty} \frac{i^k D_k}{k!} \frac{\partial^k}{\partial t^k} A(z, t) \\ + i\gamma \left(\int dt' R(t') |A|^2(z, t - t') + \Gamma^R(z, t) \right) A(z, t). \end{aligned} \quad (6)$$

Here, D_k are the dispersion coefficients, γ is the nonlinear coefficient (which depends on the nonlinear index and the geometry of the fiber). The kernel $R(t)$ is conventionally expressed as $R(t) = (1 - f_R)\delta(t) + f_R h_R(t)$ where f_R is the Raman fraction (0.18 in silica) and h_R is the phonon response function, typically approximated as $h_R(t) = [(\tau_1^2 + \tau_2^2)/\tau_1 \tau_2^2] \theta(t) e^{-t/\tau_2} \sin(t/\tau_1)$, where in silica $\tau_1 = 12$ fs and $\tau_2 = 32$ fs. The term Γ_R represents a driving force on the field due to Raman interactions with phonons, and is given in terms of the amplitude of each phonon $b(z, \Omega)$ at position z and frequency Ω by

$$\Gamma^R(z, t) = \int_0^{\infty} \frac{d\Omega}{2\pi} \sqrt{\hbar\Omega f_R \text{Im } h_R(\Omega)/\gamma} (b(z, \Omega) e^{-i\Omega t} + \text{c.c.}), \quad (7)$$

where c.c. denotes complex conjugation. The phonons can be seen as Gaussian uncorrelated random variables with correlations governed by the Bose-Einstein distribution.

The most famous limiting case of this general equation is the one where the phonons can be neglected and the dispersion can be approximated as purely second-order. The resulting equation $\partial_z A = -\frac{iD_2}{2} \partial_t^2 A + i\gamma |A|^2 A$ is called the nonlinear Schrödinger equation (NLSE) and has been studied for many decades in different nonlinear wave systems in optics, cold atoms, water waves, etc. In this limit, a key effect is the formation of solitons, pulses that propagate while preserving their shape due to an interplay of dispersion and nonlinearity. Effects related to solitons are still widely studied today, forming the key conceptual basis for developments in optics (e.g., lasers, information transmission systems, and frequency combs) and other fields. Due to the central role solitons play in nonlinear physics, foundational theoretical and experimental investigations were pursued of the quantum fluctuations in the solitons three decades ago, revealing intriguing quantum mechanical effects such as squeezed states of solitons, states with lower noise than the vacuum in some observables, as well as phenomena related to entanglement [42–50].

Despite these successful foundational investigations, much remains unknown when pushing these quantum optics effects to shorter pulse durations and higher powers, where the full description, given by Eqs. (6) and (7), is necessary. In this regime, a variety of new effects kick in which do not exist in the NLSE. For example, a higher-order soliton solution of the NLSE can breakup into smaller solitons, a phenomenon called soliton fission. These solitons can undergo friction due to spontaneous phonon emission (called stimulated Raman scattering), causing them to continuously redshift as they propagate. The new frequency components can mix to form higher-frequency components, with energy-momentum conservation mediated by nonlinearity and higher-order dispersion, a phe-

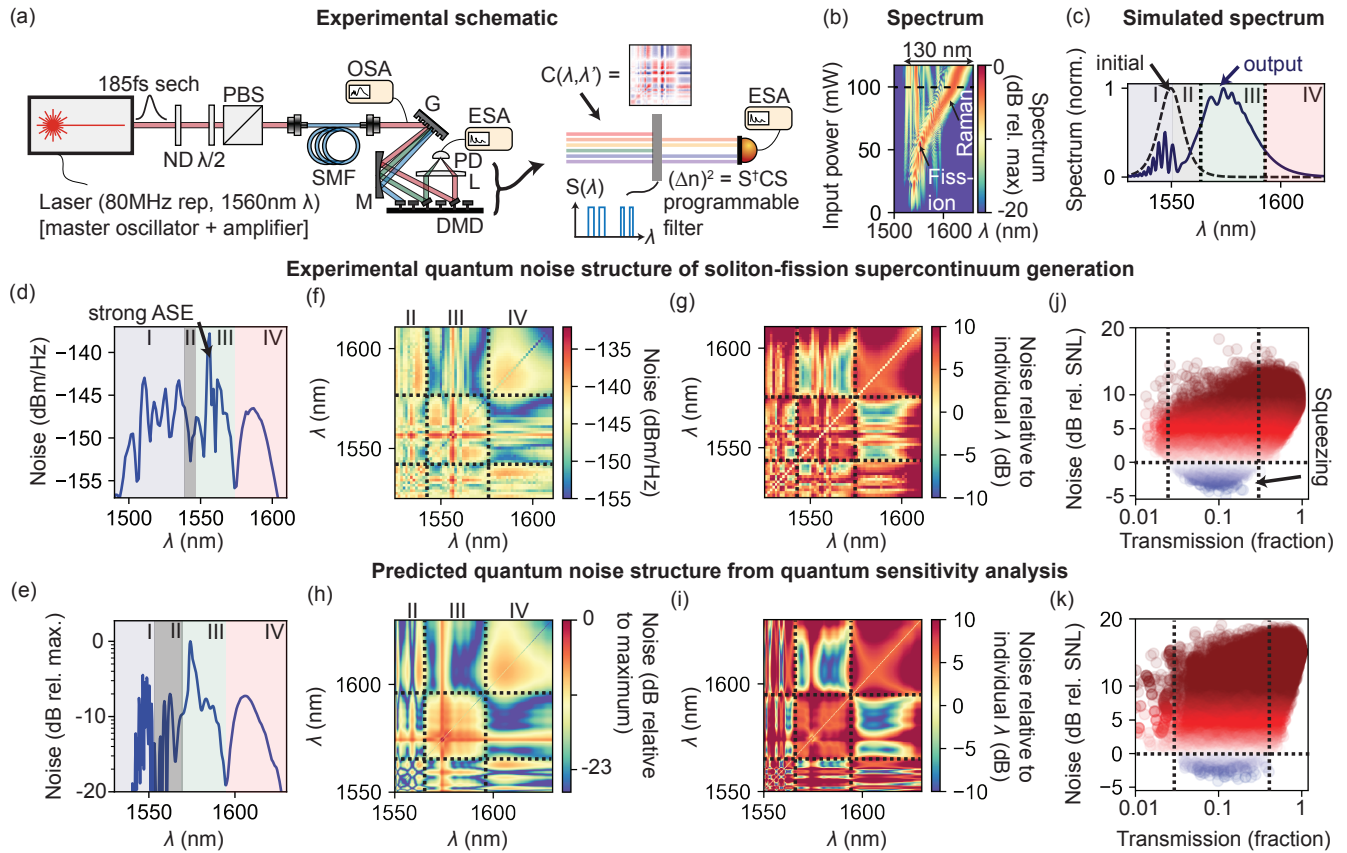


FIG. 2: Quantum optics of soliton-fission supercontinuum generation: noise, correlations, and multimode entanglement. (a) Schematic of experiment to probe quantum noise and correlations in nonlinear dynamics of intense femtosecond pulses. Light passes through a single-mode fiber (SMF; 10m length), and is then sent through a programmable spectral filter made up of a grating (G), mirror (M) and digital micromirror device (DMD). The filtered wavelengths are detected by a photodiode (PD) and intensity noise is measured with an electronic spectrum analyzer (ESA). Additional elements: filter (ND), half-wave plate ($\lambda/2$), polarizing beam splitter (PBS), lens (L), and optical spectrum analyzer (OSA). (a, Right) The programmable filter allows us to look at the noise of single wavelengths, pairs of wavelengths, and arbitrary partitions. (b) Spectrum of light passing through fiber as a function of average power, showing key signatures of soliton-fission supercontinuum generation. (c) Simulated spectrum of the output pulse for conditions similar to what will be shown in Figs. 2d,f,g,j, measured for a pulse energy of 1.25 nJ. (d,e) Noise of individual wavelengths filtered from the output, in both experiment (d) and theory (e). (f) Noise of a pair of wavelengths. Extremely low-noise pairs of wavelengths correspond to blue regions, and can have noise at or below the shot noise of the ideal coherent state, despite the individual wavelengths being much noisier, indicating strong correlation. (g) Noise of a pair, relative to the lesser of the two noises of the individual wavelengths. (h,i) Same as (f,g) but in theory. (j) Noise of an arbitrary partition of wavelengths. Scatter plot shows the noise after going through a filter that cuts out the blue and red portions of the spectrum, but is otherwise random, for 40,000 different filters. For a range of transmitted powers, noise below the shot-noise level, or intensity squeezing can be realized, indicating multimode entanglement, in good agreement with theory (k). The small deviation in the center wavelength between theory and experiment is to be expected from the error-bar of the custom spectrometer.

nomenon called dispersive wave generation. These phenomena together are known to be key physical ingredients in the important nonlinear phenomenon of supercontinuum generation, an effect in which a narrow-band input pulse, after nonlinear propagation, becomes extremely broadband [51]. As a point of terminology, when the supercontinuum generation is initiated by soliton fission, we call it soliton-fission supercontinuum generation. While much of the quantum description of supercontinuum generation has not been worked out, it is of key importance because it is known from seminal experiments that supercontinuum is a strongly noise-sensitive process [52, 53]. In particular, even when the only noise on the

pulses are quantum vacuum fluctuations (i.e., the pulses are in coherent states), the different spectral components of the output pulses can have far higher levels of noise. This quantum noise amplification has been cited as leading to phenomena such as rogue-waves in optics [54], as well as noise limits in applications such as optical coherence tomography [55].

We developed high-resolution measurements (1 nm resolution) of the frequency-resolved quantum noise of high power pulses undergoing supercontinuum generation as described by Eqs. (6) and (7). Compared to previous probes of frequency-resolved statistics in supercontinuum generation [47, 56, 57], our system is characterized by simultaneously high resolu-

tion and quantum-level sensitivity. Fig. 2a depicts the experiment: we pass femtosecond pulses through a single-mode silica fiber, leading to soliton-fission supercontinuum generation. In Fig. 2b, we show the spectrum of the light exiting the fiber as a function of the average power of the pulses. The spectra show the characteristic features of supercontinuum generation: strong spectral broadening, soliton fission, strong Raman, and generation of blue-shifted frequencies with respect to the center wavelength of the pump. These features are also seen in simulations, as shown in Fig. 2c where we show the simulated spectrum for a fixed average power. There, we also conceptually divide the spectrum into four regions: I. the blue-side of the pump wavelength, II. the blue side of the Raman soliton (the red-shifted peak), III. the peak of the Raman soliton, and IV. the red side of the Raman soliton. These four regions have qualitatively different behaviors, and the entanglement and correlation that we observe will be connected to the boundaries between these regions.

We now probe the spectral quantum noise structure of the output light for this same fixed power (100 mW average power, equivalently 1.25 nJ pulse energy). To do so, we pass the light exiting the fiber through a programmable spectral filter which allows us to send any part of the spectrum into a photodiode and measure noise. Passing one narrow band of wavelengths allows us to measure the photon-number variance (noise) of different wavelengths: $(\Delta n_\lambda)^2$. Passing two distinct narrow bands of wavelengths probes the photon-number variance of a two-mode state composed of wavelengths $[\Delta(n_\lambda + n_{\lambda'})]^2$, which we refer to as “pair noise.” Passing many wavelengths will reveal yet different noise. Different subsets of wavelengths have different photon-number variances because of correlations between different wavelengths (as shown in Fig. 2(a), right). In particular, the variance in a sum of wavelengths is given by $(\Delta[\sum_\lambda n_\lambda])^2 = \sum_\lambda (\Delta n_\lambda)^2 + \sum_{\lambda \neq \lambda'} C(\lambda, \lambda')$, where $C(\lambda, \lambda') = \langle \delta n_\lambda \delta n_{\lambda'} \rangle$ is the number-number correlation function.

The wavelength-dependent noises are shown in Fig. 2d. While they have a variety of complex features, and very strong orders-of-magnitude variations, we can interpret the results by making use of the theoretical calculation of the noise according to quantum sensitivity analysis (Fig. 2e), as well as the spectrum of Fig. 2c, which line up well with the data. The combination of experiment and theory allows us to draw the following conclusions. The output noises deviate strongly from what one expects if the output were in a coherent state, where each wavelength would have shot-noise level of fluctuations (compare Figs. 2c and 2e). In that case, the noise would be proportional to the intensity. In contrast, the noises in region I and IV have very high noise relative to their spectral intensities. The IV region features a strong quantum noise peak even when the spectrum shows no such peak. As will be elaborated later, the noise at these wavelengths is suggested by theory to be 100-times the shot-noise limit, corresponding to a strong amplification of quantum noise (Fig. 3a).

Meanwhile, the lowest noise tends to be in the region III overlapping with the peak of the red-shifted part of the spectrum (called the Raman soliton), ignoring the strong peak attributed to amplified spontaneous emission of the incident

laser. The boundaries of the regions labeled II/III and III/IV in Figs. 2c present the lowest noises. These points are in good correspondence with the inflection points of the Raman soliton spectrum. As our theoretical analysis shows, it is these two wavelengths that appear to have noise levels essentially at the shot noise level (according our theory, these points can also be below the shot noise level).

Having shown the quantum noise structure of the individual wavelengths, we now probe the noise of multi-wavelength states based on two or more wavelengths at a time. Fig. 2f shows the noise associated with pairs of wavelengths. Due to correlations between wavelengths, the noise of a pair of wavelengths $[\Delta(n_\lambda + n_{\lambda'})]^2$ can be strongly enhanced (red regions) or suppressed (blue) relative to the individual wavelengths. In Fig. 2g, we show how the noise of a pair $[\Delta(n_\lambda + n_{\lambda'})]^2$ compares to the lower of the individual variances $(\Delta n_\lambda)^2$, $(\Delta n_{\lambda'})^2$. In the blue regions, the noise can be about an order of magnitude (maximum 8 dB lower in the III/IV boundary region), lower than at the individual wavelengths. The correlated low-noise regions form a ring around the outer perimeter of the III-III region denoted in Figs. 2f,g (the regions correspond to the same wavelengths as for the individual noises), with no lower-noise pairs in the III-III or IV-IV regions. These experimental observations are in good agreement with the predictions of quantum sensitivity analysis, shown in Figs. 2h,i, which shares many features in common with the Fig. 2f.

The results of Figs. 2f-i directly show that much of the high noise in supercontinuum is tied up in correlations: for many wavelengths, there is a partner wavelength for which the collective noise is far lower. Motivated by this, we then looked at the noise associated with more complex multi-wavelength states, composed of more than two wavelengths. Fig. 2j shows the result of an experiment in which we measure the noise of different subsets of the output spectrum passed through by our programmable filter in Fig. 2a (40,000 different subsets), and measure the noise. In this case, we measured the power associated with each subset of wavelengths, which allows us to plot the noise relative to the shot noise limit. The color of each point is based on the y-axis value, and the x-axis value represents the fraction of the output power carried by the subset, normalized to the total output power. As Fig. 2j shows, there is a region between 3% and 30% transmission where some of the multi-wavelength states have noise below the shot noise limit, corresponding to intensity squeezing. The maximum intensity squeezing is 4.2 dB below the shot-noise limit, limited by linear loss associated with our setup (the maximum squeezing without linear loss is expected to be around 9 dB from our theory). The measured squeezing is also reproduced by our theory in both the magnitude and location (on the x-axis). This squeezing is significant for several reasons. For one, it lies in stark contrast to the conventional picture of soliton-fission supercontinuum generation, which is considered to be noise-amplifying, and turning clean coherent states into noisy outputs. Here, we find that by looking at the right sets of wavelengths, one instead sees noise below the coherent state level, which is a genuinely quantum effect in a system which has been considered only classically in the vast majority of studies. Moreover, our finding is significant because the

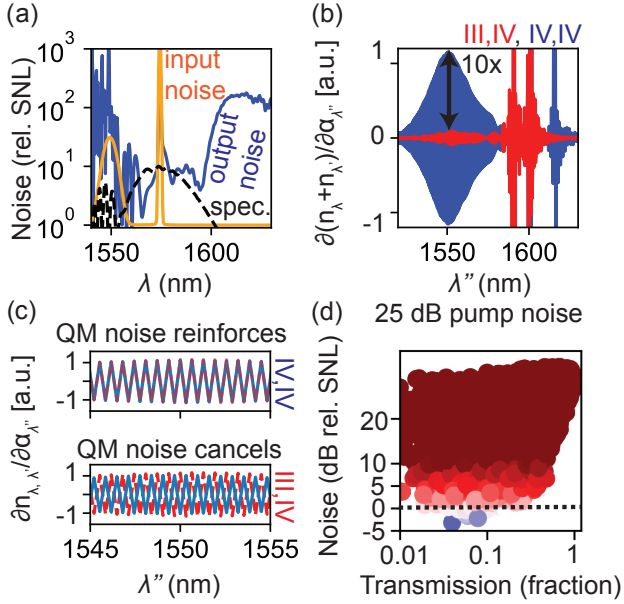


FIG. 3: Unraveling complex quantum noise dynamics in soliton-fission supercontinuum, through quantum sensitivity analysis. (a) Noise of individual wavelengths relative to shot noise (blue), compared to the initial excess noise distribution (orange). The output spectrum is overlaid in black (arbitrary units). (b) Quantum sensitivity analysis of pair noise for a pair in the III-IV versus IV-IV regions defined in Fig. 2c. Pairs in the low noise III-IV region are strongly insensitive to vacuum fluctuations, which is explained in (c) where we see that vacuum fluctuations cause the two wavelengths to shift in opposite directions. In contrast, the wavelengths in the IV-IV region shift in the same direction. (d) Noise of multi-wavelength subsets as in Figs. 2j,k, but now assuming the initial pulse is 25 dB above the shot noise level. Squeezing of the same magnitude is still attainable.

squeezing indicates the existence of quantum entanglement between different colors generated in the process.

Having shown the experiments, and the excellent correspondence with our predictions from quantum sensitivity analysis, we now turn to developing a mechanistic interpretation of these phenomena using our framework. By doing this, we will be able to determine which vacuum fluctuations have the biggest impact on the outputs. Let us start with the noises of individual wavelengths. In what follows, we will switch from labeling colors by wavelength λ to labeling them by frequency ω . We will also suppress the “in” and “out” labels introduced in Section I. The intensity noise of a single frequency ω is given from a quantum sensitivity analysis of Eqs. (6-7) by:

$$(\Delta n_\omega)^2 = \int \frac{d\omega'}{2\pi} \left| \frac{\partial n_\omega}{\partial \alpha_{\omega'}} \right|^2 F_{\omega'} + \int dz \frac{d\Omega}{2\pi} \left| \frac{\partial n_\omega}{\partial b_{\Omega,z}} \right|^2 F_{\Omega,z}, \quad (8)$$

where $\alpha_{\omega'}$ is the complex amplitude of the Fourier component of the input pulse at frequency ω' , $F_{\omega'} = \langle \delta a_{\omega'} \delta a_{\omega'}^\dagger + \delta a_{\omega'}^\dagger \delta a_{\omega'} \rangle$ is the excess noise of frequency ω' relative to the shot noise level. In Fig. 3a, we show the excess noise distribution of the input as a function of wavelength (orange

curve), showing strong excess noise near the input wavelengths. Meanwhile, $b_{\Omega,z} = b(z, \Omega)$ is the complex amplitude of a phonon of frequency Ω and position z defined in Eq. (7), and $F_{\Omega,z} = 2n_{\Omega,z} + 1$ is the excess noise of that phonon, which in thermal equilibrium, is set by the Bose-Einstein factor $n_{\Omega,z} = [e^{\hbar\Omega/k_B T} - 1]^{-1}$, where \hbar is Planck’s constant, k_B is Boltzmann’s constant and T is temperature. While we have included the phonon degrees of freedom for generality, their influence on the observables in Fig. 3 is weak, with the main influence of the phonons coming from the convolution term in Eq. (6). Fig. 3a shows the noise of the individual wavelengths relative to shot noise. As can be seen, the noise gets strongly amplified near the pump wavelengths (near 1550 nm) and at the tail of the Raman soliton (above 1600 nm). Meanwhile, there appear to be wavelengths near the shot noise slightly on the blue and red-detuned sides of the peak of the Raman soliton. We note that despite the large excess noise of the peak, there can be wavelengths much closer to the shot noise level. According to Eq. (8), this must happen when the output intensity changes only weakly when input wavelengths near the pump change (due to quantum or other fluctuations). In the SI, we show this indeed happens.

Now let us understand the low pair-noise states of Figs. 2f-i. Ignoring phonons (see SI for full expression), the noise of a pair of frequencies is given by

$$\Delta(n_\omega + n_{\omega'})^2 = \int \frac{d\omega''}{2\pi} F_{\omega''} \left(\left| \frac{\partial n_\omega}{\partial \alpha_{\omega''}} \right|^2 + \left| \frac{\partial n_{\omega'}}{\partial \alpha_{\omega''}} \right|^2 \right) + \int \frac{d\omega''}{2\pi} F_{\omega''} 2\text{Re} \left[\frac{\partial n_\omega}{\partial \alpha_{\omega''}} \frac{\partial n_{\omega'}}{\partial \alpha_{\omega''}^*} \right]. \quad (9)$$

In Fig. 3b, we show the integrand of Eq. (9) for two different pairs, one in the low-noise III-IV region (red), and one in the high-noise IV-IV region (blue). Each value on the plot represents the contribution of a vacuum fluctuation to the pair noise as a function of wavelength on the x -axis. The main feature to focus on is the contribution of the pump wavelengths (within 10 nm of 1550 nm). For a pair in the III-IV region, the contribution of vacuum fluctuations at the pump wavelength is over an order of magnitude smaller than the contribution for a pair in the IV-IV region. Fig. 3c elucidates this point by zooming in to wavelengths near the pump, and showing the individual shifts of n_λ and $n_{\lambda'}$ in response to vacuum fluctuations. For a pair in the IV-IV region, a vacuum fluctuation at the pump shifts n_λ and $n_{\lambda'}$ in the same direction, leading to enhanced noise. In contrast, the pair n_λ and $n_{\lambda'}$ in the III-IV region shift in the opposite direction in response to vacuum fluctuations, leading to smaller shifts in $n_\lambda + n_{\lambda'}$. The lowest noise points correspond to those for which n_λ and $n_{\lambda'}$ shift in exact opposition to vacuum fluctuations. Moreover, it is clear that the low noise at the III-IV region is robust to added noise at the pump, since the pump contribution to the overall noise is very small in the first place. This noise robustness can be extremely potent, as we show for the example of the multi-wavelength squeezing experiments. In Fig. 3d, we show that even when the initial pulses are 700 times above the shot noise level, squeezing can still be achieved. This is remarkable in light of the conventional wisdom that strong excess noise precludes squeezing. To summarize Fig. 3, our theory points to

a strong noise-robustness of the low-noise states we observed. This also lies in contrast to the picture of soliton-fission supercontinuum generation as noise-sensitive.

To summarize this section, we put forth a new picture of soliton-fission supercontinuum generation as a process which leads to a strong buildup of entanglement, that manifests as noise amplification when looking at one wavelength at a time. The low-noise and noise-robust multi-wavelength states we found are tied to low-noise wavelengths that form around the inflection points of the Raman soliton, and the low-noise multi-wavelength states arise from a very strong cancellation of vacuum fluctuations for wavelengths on opposite sides of these inflection points.

III. NEW CONCEPTS FOR CONTROLLING QUANTUM NOISE

Having shown how quantum sensitivity analysis enables new insights in complex experiments, we now present a few new concepts for controlling quantum noise that follow from our framework of quantum sensitivity analysis. We also show one example which does not involve light, to show the generality of our framework for problems beyond nonlinear optics.

A. Broadband quantum noise suppression using femtosecond squeezed light

As described in the previous section, in frequency conversion phenomena like supercontinuum generation, the new wavelengths generated are noisy due to amplification of quantum fluctuations. While the use of correlations and multi-wavelength states enables much lower noise, it is also of interest to lower the noise of individual wavelengths. We now show from quantum sensitivity analysis how this can be done. The results we show represent one of the first proposals for using ultrafast squeezed light to improve an optical device.

We will consider a simpler nonlinear system which contains similar physics but can be understood almost analytically: a nonlinear medium with negligible temporal dispersion such that a pulse passing through it undergoes only self-phase modulation. The classical description of the evolution of the electric field envelope of the pulse, $A(z, t)$ is given as $\partial_z A(z, t) = i\gamma|A(z, t)|^2 A(z, t)$. The pulse after a length L of propagation, $A(L, t)$ is given in terms of the incident pulse envelope $A(0, t)$ as $A(L, t) = e^{i\theta|A(0, t)|^2} A(0, t)$, with $\theta = \gamma L$. From quantum sensitivity analysis, we can now write down an expression for the noise of the number of photons at the output, $n(L, \omega)$ in a narrow band of frequencies $[\omega - \Delta\omega/2, \omega + \Delta\omega/2]$ of width $\Delta\omega$ centered around frequency ω . Classically, $n(L, \omega) = \int_{\omega - \Delta\omega/2}^{\omega + \Delta\omega/2} \frac{d\omega}{2\pi} |A(L, \omega)|^2$. The

variance of $n(L, \omega)$ is given by

$$(\Delta n(L, \omega))^2 = \int ds (2N(s) + 1) \left| \frac{\partial n(L, \omega)}{\partial A(0, s)} \right|^2 + 2\text{Re} \left[P(s) \left(\frac{\partial n(L, \omega)}{\partial A(0, s)} \right)^2 \right]. \quad (10)$$

An expression for the derivative in question is given in the SI, Section V. B. The quantities $N(s), P(s)$ capture the fluctuations of the different time-slices of the incident pulse. In particular: $\langle \delta A(s) \delta A^\dagger(s') \rangle = \delta(s - s') N(s)$, while $\langle \delta A(s) \delta A(s') \rangle = \delta(s - s') P(s)$.

We will now show that by controlling the input fluctuations $N(s), P(s)$, it is possible to strongly lower the noise of all of the wavelengths, by nearly an order of magnitude. Consider the system in Fig. 4a: a beamsplitter is illuminated with an intense coherent input on one end (left) and pulsed squeezed vacuum (top). The pulsed squeezed vacuum can be generated by sending a pulse through a nonlinear medium, as has been realized in early experiments on squeezing in fibers [1]. We consider the case where the squeezed pulse is generated using self-phase modulation of a pulse through a fiber with nonlinear coefficient γ' and length ℓ with an incident pulse of amplitude $\beta(s)$. It then follows that $N(s) = |\zeta(s)|^4$, $P(s) = (1 + i|\zeta(s)|^2) i\zeta(s)^2 e^{2i|\zeta(s)|^2}$. Here, $\zeta(s) \equiv \sqrt{\chi} \beta(s)$, with $\chi = \gamma' \ell$. Further, we note that $\beta(s) = |\beta(s)| e^{i\varphi(s)}$, with $\phi(s)$ being the phase of each time-slice of the pulse incident into the squeezer.

In Fig. 4b, we show the classical expectation for the spectrum of a gaussian pulse (185 fs FWHM) undergoing self-phase modulation. The amplitude of the incident pulse (the coherent part, after the beamsplitter) is chosen such that the nonlinear phase shift of the peak of the pulse is 20π , leading to a large spectral broadening. In Fig. 4c, we see that relative to shot noise, the noise of the individual wavelengths generated is far above the shot-noise level (nearly 100-times), despite the individual wavelengths at the input being shot-noise limit, analogous to the situation described in the previous section (this effect is very general). On the other hand, when injecting a squeezed pulse into the upper port of the beamsplitter in Fig. 4(a), the noise of the individual wavelengths can be brought down by nearly an order of magnitude, and in a nearly wavelength-independent manner.

We now use the quantum sensitivity analysis expression of Eq. (10) to account for the large bandwidth of the effect. It can be understood by approximating Eq. (10) as $\int ds (2N(s) + 2\text{Re} P(s) + 1) \left| \frac{\partial n(L, \omega)}{\partial A(0, s)} \right|^2$ [102]. From this approximation, one sees that since $\text{Re} P(s)$ can be negative, $(2N(s) + 2\text{Re} P(s) + 1)$ can be below 1, therefore reducing the fluctuations below what one gets from a coherent state input. Moreover, the effect is essentially independent of ω , as the factor $(2N(s) + 2\text{Re} P(s) + 1)$ has no ω dependence. From this explanation, the effect can be understood as the result of reducing the relevant vacuum fluctuations which seed the frequency-generation process.

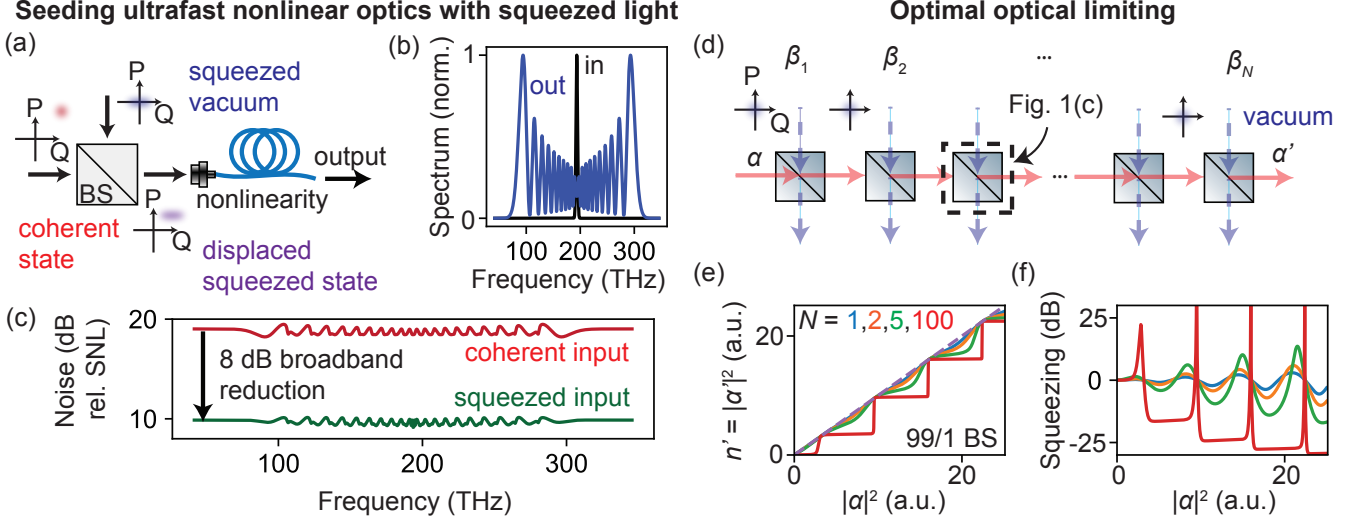


FIG. 4: **New concepts for controlling quantum noise of light.** (a-c) Driving ultrafast nonlinear phenomena with squeezed femtosecond pulses. (a) Concept for lowering the noise of individual wavelengths generated in a frequency-broadening process. By seeding a frequency-broadening phenomenon (such as supercontinuum generation) with a displaced-squeezed pulse (realized by mixing a coherent state and squeezed state via a beamsplitter), the noise of the individual wavelengths can be strongly reduced. (b) Mean number of photons in each frequency after self-phase modulation of a 150 fs gaussian pulse. (c) Noise of individual wavelengths for coherent versus coherent-squeezed pulses of the same intensity, showing a ~ 10 dB broadband noise reduction of each wavelength. Parameters provided in SI. (d-f) Optimal optical limiting. (d) A chain of nonlinear Mach-Zehnder interferometers similar to than in Fig. 1c. (e) Transmission and (f) squeezing for different input intensities. The nonlinear transmission takes the form of a series of plateaus with discrete output photon numbers. Meanwhile, the squeezing displays a series of “stop bands” where the intensity noise is extremely low over a wide range of input powers.

B. Optimal optical limiting

The second example follows on the discussion of Sec. IA. We show how to go beyond the maximal squeezing of a single interferometer, and how to realize it over a broad range of powers. Consider the cascaded nonlinear Mach-Zehnder interferometer of Fig. 4d: it is constructed by feeding the output of the α' port of the i interferometer into the α port of the $i+1$ interferometer. Vacuum enters the β ports of each interferometer [103]. This time, each interferometer being 90/10 is no longer optimal. Taking all of the beamsplitters to be the same, ratios closer to 100/0 lead to much better results. The transmission and squeezing are shown in Figs. 4e,f. The transmission shows a distinct staircase structure where different input intensities get mapped to a discrete set of output intensities. These plateaus correspond to extremely wide and deep squeezing regions, which, for the same intensities as in Figs. 1(d-e), give squeezing values as high as 30 dB. The existence of low noise also exists over a far wider range of powers than the single interferometer (of any length).

The reason the noise reduction is so effective is as follows: at each beamsplitter, vacuum fluctuations are introduced. From quantum sensitivity analysis, one finds that the added fluctuations go as (see SI)

$$(\Delta n_{i+1})^2 = (1 - 2L'(n_i))(\Delta n_i)^2 + L(n_i), \quad (11)$$

where $L(n) = 4n\epsilon^2 \cos^2(n\theta/2)$. The first term is the classical optical limiting term discussed in Sec. IIA, while the second term is the contribution from vacuum fluctuations at

the i th beamsplitter in Fig. 4d. As can be seen, there are certain values of n_i (the mean number of photons at the i th stage) where $L(n_i) = 0$ and the contribution from vacuum fluctuations vanishes. Meanwhile, the first term goes to zero more slowly, causing the fluctuations to decrease with negligible addition of vacuum noise, until the intensity fluctuations reach absolute zero (in the limit of infinitely many splitters). This analysis shows that by designing architectures that adiabatically add vacuum fluctuations, it is possible in principle to go far beyond the limits of existing squeezing architectures. We also note that in the SI, we show that these same architectures also enable generating important quantum states beyond squeezed states, such as propagating photonic Fock states (eigenstates of the photon number operator), which have long been desired but are not currently possible to deterministically generate. While such states go beyond the scope of our current framework, it shows that the design concepts emerging from quantum sensitivity analysis have a broad applicability to generating useful quantum mechanical states.

C. Nonlinear control of lattice fluctuations in solids

In this section, we consider an example outside of nonlinear optics, to show the applicability of our framework to general nonlinear systems. The example we choose is motivated by recent developments in the field of phononics. There, strong terahertz (THz) or mid-IR pulses have been used to drive lattice vibrations in polar materials with infrared-active

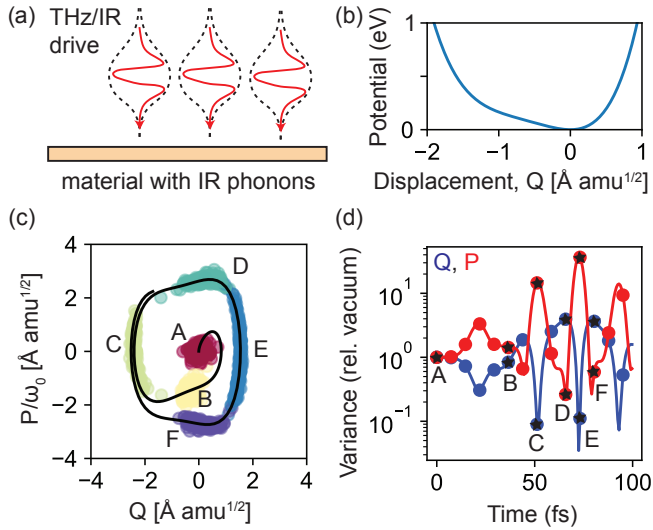


FIG. 5: Squeezing and correlations in nonlinear dynamics of light-driven phonons. (a) A few-cycle terahertz pulse incident in a material can resonantly excite a phonon mode, causing displacement of the atoms in the lattice. Example here is LiNbO_3 . (b) Potential energy as a function of modal displacement Q (in conventionally used dimensions of length \times mass $^{1/2}$). Q is defined such that the displacement of ion i is $Q\eta_i$, where η_i is a unit vector. For large displacements, the potential deviates strongly from the harmonic approximation typically used to describe phonon dynamics. (c) Dynamics of the modal displacement and the conjugate modal momentum ($P = \dot{Q}$), with ω_0 being the phonon frequency in the harmonic approximation. Black line indicates mean trajectory. Red dots represent a cluster of initial conditions, and dots of different colors represent how those initial conditions evolve over time (letters have the same meaning in (c) and (d)), showing the spread of (quantum) fluctuations in the initial conditions. (d) Variance of modal displacement and momentum, calculated according to Eq. (13), showing large degrees of squeezing of the modal displacement (above 10 dB), resulting from a strong insensitivity of the displacement to the initial conditions for certain times. The driving pulse is taken to be $E(t) = E_0 \sin(\omega_d t) e^{-t^2/\tau^2}$, with $E_0 = 100 \text{ MV/cm}$, $\omega_d = 2\pi \times 17.5 \text{ THz}$, and $\tau = 150 \text{ fs}$.

phonons. Due to advances in the generation of intense IR/THz fields, it is possible to drive the atoms of the lattice (which can be thought of as masses attached by springs) to displacements where Hooke's law no longer holds, and the atoms undergo nonlinear dynamics [58]. In this nonlinear phononic regime, analogs of nonlinear optics phenomena have been shown, such as upconversion and downconversion of vibrational modes [59, 60]. Recently, these nonlinear upconversion effects have been taken into a nonperturbative regime, generating as many as five harmonics of the driving field, analogous to the phenomenon of high-harmonic generation in optics.

The vast majority of the analysis in this field has been classical, focusing on the mean amplitude of the atomic vibrations, but the fluctuation properties are also important from a condensed matter perspective, as the fluctuations are relevant to the phases mediated by vibrations, such as magnetism, ferroelectricity, and potentially superconductivity [61–64]. Our framework directly connects the existing classical models and

the quantum fluctuations, allowing us to take the existing classical models and make new predictions. We show this in Fig. 5, where we consider a material (here, LiNbO_3) in the presence of a strong mid-IR drive which excites an optical phonon of frequency 15 THz. The optical phonon corresponds to a displacement of the i th atom of each unit cell, which is typically parameterized by $Q\eta_i$, where η_i is an atom-dependent unit-vector. Q is given in dimensions of length \times mass $^{1/2}$ such that the potential energy in the harmonic approximation is $U(Q) = \frac{1}{2}\omega_0^2 Q^2$, with ω_0 the phonon frequency. When the displacement of the atoms is sufficiently large, the potential becomes significantly anharmonic, leading to nonlinear response such as frequency upconversion. In LiNbO_3 , the potential is well-approximated by $U(Q) = \frac{1}{2}\omega_0^2 Q^2 + \frac{1}{3}a_3 Q^3 + \frac{1}{4}a_4 Q^4 + \frac{1}{5}a_5 Q^5$, and is shown in Fig. 5(b) (all parameters are taken from [59]). Classically, the dynamics of the modal displacement and modal momentum P , in the presence of a driving field $E(t)$, are given by

$$\begin{aligned}\dot{Q} &= P \\ \dot{P} &= -\nabla U + Z^* E(t),\end{aligned}\quad (12)$$

where Z^* is an effective charge ($Z^* = 1e/\sqrt{\text{amu}}$, where e is the electron charge and amu is the atomic mass unit) [104]. To determine the dynamics of quantum fluctuations in some quantity X (e.g., $X = Q, P$), quantum sensitivity analysis gives this as (see SI)

$$\begin{aligned}(\Delta X)^2 &= \left(\frac{\partial X}{\partial Q_0}\right)^2 (\Delta Q_0)^2 + \left(\frac{\partial X}{\partial P_0}\right)^2 (\Delta P_0)^2 \\ &\quad + \frac{\partial X}{\partial Q_0} \frac{\partial X}{\partial P_0} (\langle Q_0 P_0 + P_0 Q_0 \rangle - 2\langle Q_0 \rangle \langle P_0 \rangle),\end{aligned}\quad (13)$$

where the zero subscript denotes initial time quantities. For the standard case of vacuum fluctuations around zero position and momentum, we have $(\Delta Q_0)^2 = \hbar/2\omega$, $(\Delta P_0)^2 = \hbar\omega/2$, and $\langle Q_0 P_0 + P_0 Q_0 \rangle - 2\langle Q_0 \rangle \langle P_0 \rangle = 0$. In other words, the noise of quantities like Q, P are governed by the sensitivity of the classical trajectories to the initial conditions. The classical trajectories associated with various initial conditions are shown in Fig. 5(c), and show the existence of certain times for which the variance of Q or P can be quite below the standard quantum limit. Examining the mean trajectory (in black), it is clear why this can happen. The mean trajectory has a quasi-rectangular shape. In the relatively flat regions, either Q or P hardly changes over time. For example, around the region in phase space near time C, Q hardly changes with time. Given that a time-delay (or phase lag) is similar to a change in initial conditions, this indicates that different initial conditions lead to minimal changes in Q , leading to lower noise than the standard vacuum level. This is shown in Fig. 5(d) where using quantum sensitivity analysis, we find certain times for which the lattice fluctuations can be suppressed by over ten times the vacuum level. There are also times for which fluctuations in the modal momentum can be very large, and as large as the mean values themselves, indicating the buildup of macroscopic fluctuations.

These results are interesting in light of the fact that substantial phonon squeezing has yet to be measured, but may already

be present in existing experiments. This would also give a route to generate squeezed *light* at mid-IR and THz frequencies, where squeezed sources have not been developed. THz light generation would be achieved by exploiting the coupling of these IR-active phonons to light, manifesting as phonon polaritons which could be outcoupled to the far-field. These results are also interesting given that generally, high-harmonic-generation as a route to squeezing has not been looked at, as it is typically assumed that one would need a parametric interaction or a Kerr interaction to squeeze [23]. Nevertheless, we can understand this effect from the perspective of quantum sensitivity analysis. This can be seen most easily at the time points C and E, where the classical trajectory changes in momentum rapidly over a relatively short period of time. We emphasize that this perspective of quantum sensitivity analysis not only makes clear the physics in a way that a standard approach does not, but it also indicates a clear classical guideline to reducing the fluctuations further. For example, by engineering the driving field to induce a more rectangular trajectory, fluctuations could be suppressed further. Moreover, in settings involving multiple phonon modes, or polaritonic effects, our framework is the only one that can currently deal with the dimensionality of the resulting model.

IV. OUTLOOK

Summarizing, we have developed and experimentally validated a new framework, quantum sensitivity analysis, for predicting the dynamics of quantum noise in nonlinear systems. The framework enables a completely new way to address the response of complex systems to quantum fluctuations, by performing sensitivity analysis on the corresponding classical theory. By using this framework, we were able to derive a wide variety of new results related to controlling noise, primarily in optics, leading to new concepts for quantum light generation, for creating ultra-broadband and ultra low-noise light sources, and for understanding complex experiments. Our theory also enabled shedding light on a surprising set of low-noise and noise-robust states seen that we observed in experiments probing the physics of supercontinuum generation. We believe that the framework advanced here should immediately enable a variety of breakthroughs in understanding the fundamental quantum description of many complex nonlinear systems, which have proved difficult to probe via the conventional theoretical tools.

We briefly outline a few directions which are natural from our framework. In general, the area of “quantum effects in nonlinear systems” is wide open for discovery. In the context of nonlinear optics, there is a huge range of effects which are being investigated, whose “quantum optical nature” has not been touched and could engender a new generation of low-noise and high-power laser systems which could enable extending quantum optics to new domains. Examples of such systems and effects include complex parametric oscillators [65–67], integrated squeezed light sources [68–72], nonlinear PT-symmetric systems [73, 74], topological solitons [75–77], self-similar systems [78, 79], disordered systems [80, 81], spatially multimode nonlinear fibers [82–88], soliton microcombs [89–91], topological lasers [92, 93], and high-harmonic generation [94, 95].

Beyond nonlinear optics, analogues of nonlinear optics have emerged in several areas of condensed matter physics. Examples include light-driven phonons discussed in the previous section, as well as magnons [96, 97] and excitons in quantum wells [98, 99]. Each have pronounced classical nonlinear interactions that can lead to control over the fluctuations. The manipulation of fluctuations in these material systems have exciting prospects for stabilizing material phases as well as new routes to generating quantum states of light and materials. In general our framework will enable the design of optimal architectures for these systems as well.

V. ACKNOWLEDGEMENTS

We acknowledge useful discussions with Erich Ippen, Ido Kaminer, Logan Wright, Dominik Juraschek, Ryotatsu Yanagimoto, Tatsuhiro Onodera, and Frank Wise. N.R. acknowledges the support of a Junior Fellowship from the Harvard Society of Fellows. Y. S. acknowledges support from the Swiss National Science Foundation (SNSF) through the Early Postdoc Mobility Fellowship No. P2EZP2-188091. J.S. acknowledges previous support of a Mathworks Fellowship, as well as previous support from a National Defense Science and Engineering Graduate (NDSEG) Fellowship (F-1730184536). This material is based upon work also supported in part by the U. S. Army Research Office through the Institute for Soldier Nanotechnologies at MIT, under Collaborative Agreement Number W911NF-23-2-0121. We also acknowledge support of Parviz Tayebati.

-
- [1] Hermann A Haus. *Electromagnetic noise and quantum optical measurements*. Springer Science & Business Media, 2000.
- [2] A gravitational wave observatory operating beyond the quantum shot-noise limit. *Nature Physics*, 7(12):962–965, 2011.
- [3] Lisa Barsotti, Jan Harms, and Roman Schnabel. Squeezed vacuum states of light for gravitational wave detectors. *Reports on Progress in Physics*, 82(1):016905, 2018.
- [4] Michael A Taylor, Jiri Janousek, Vincent Daria, Joachim Knittel, Boris Hage, Hans-A Bachor, and Warwick P Bowen. Biotical measurement beyond the quantum limit. *Nature Photonics*, 7(3):229–233, 2013.
- [5] Catxere A Casacio, Lars S Madsen, Alex Terrasson, Muhammad Waleed, Kai Barnscheidt, Boris Hage, Michael A Taylor, and Warwick P Bowen. Quantum-enhanced nonlinear microscopy. *Nature*, 594(7862):201–206, 2021.
- [6] Y Yamamoto and HA Haus. Preparation, measurement and information capacity of optical quantum states. *Reviews of Modern Physics*, 58(4):1001, 1986.

- [7] Carlton M Caves and Peter D Drummond. Quantum limits on bosonic communication rates. *Reviews of Modern Physics*, 66(2):481, 1994.
- [8] Yoshihisa Yamamoto, Susumu Machida, and Wayne H Richardson. Photon number squeezed states in semiconductor lasers. *Science*, 255(5049):1219–1224, 1992.
- [9] Tobias Herr, Klaus Hartinger, Johann Riemensberger, Christine Y Wang, Emanuel Gavartin, Ronald Holzwarth, Michael L Gorodetsky, and Tobias J Kippenberg. Universal formation dynamics and noise of kerr-frequency combs in microresonators. *Nature photonics*, 6(7):480–487, 2012.
- [10] Chengying Bao, Myoung-Gyun Suh, Boqiang Shen, Kemal Safak, Anan Dai, Heming Wang, Lue Wu, Zhiqian Yuan, Qi-Fan Yang, Andrey B Matsko, et al. Quantum diffusion of microcavity solitons. *Nature Physics*, 17(4):462–466, 2021.
- [11] Andrea C Triscari, Aleksandr Tusnin, Alexey Tikan, and Tobias J Kippenberg. Quiet point engineering for low-noise microwave generation with soliton microcombs. *arXiv preprint arXiv:2306.08580*, 2023.
- [12] Johannes Franke, Sean R Muleady, Raphael Kaubruegger, Florian Kranzl, Rainer Blatt, Ana Maria Rey, Manoj K Joshi, and Christian F Roos. Quantum-enhanced sensing on optical transitions through finite-range interactions. *Nature*, 621(7980):740–745, 2023.
- [13] William J Eckner, Nelson Darkwah Oppong, Alec Cao, Aaron W Young, William R Milner, John M Robinson, Jun Ye, and Adam M Kaufman. Realizing spin squeezing with rydberg interactions in an optical clock. *Nature*, 621(7980):734–739, 2023.
- [14] John M Robinson, Maya Miklos, Yee Ming Tso, Colin J Kennedy, Tobias Bothwell, Dhruv Kedar, James K Thompson, and Jun Ye. Direct comparison of two spin-squeezed optical clock ensembles at the 10- 17 level. *Nature Physics*, pages 1–6, 2024.
- [15] Christian L Degen, Friedemann Reinhard, and Paola Capellaro. Quantum sensing. *Reviews of modern physics*, 89(3):035002, 2017.
- [16] Benjamin J Lawrie, Paul D Lett, Alberto M Marino, and Raphael C Pooser. Quantum sensing with squeezed light. *Ac_s Photonics*, 6(6):1307–1318, 2019.
- [17] Michael A Taylor and Warwick P Bowen. Quantum metrology and its application in biology. *Physics Reports*, 615:1–59, 2016.
- [18] R.E Slusher, LW Hollberg, Bernard Yurke, JC Mertz, and JF Valley. Observation of squeezed states generated by four-wave mixing in an optical cavity. *Physical review letters*, 55(22):2409, 1985.
- [19] Ling-An Wu, HJ Kimble, JL Hall, and Huifa Wu. Generation of squeezed states by parametric down conversion. *Physical review letters*, 57(20):2520, 1986.
- [20] Robert M Shelby, Marc D Levenson, Stephen H Perlmutter, Ralph G DeVoe, and Daniel F Walls. Broad-band parametric deamplification of quantum noise in an optical fiber. *Physical review letters*, 57(6):691, 1986.
- [21] Markus Aspelmeyer, Tobias J Kippenberg, and Florian Marquardt. Cavity optomechanics. *Reviews of Modern Physics*, 86(4):1391, 2014.
- [22] Jian Ma, Xiaoguang Wang, Chang-Pu Sun, and Franco Nori. Quantum spin squeezing. *Physics Reports*, 509(2-3):89–165, 2011.
- [23] Michael Knap, Mehrtash Babadi, Gil Refael, Ivar Martin, and Eugene Demler. Dynamical cooper pairing in nonequilibrium electron-phonon systems. *Physical Review B*, 94(21):214504, 2016.
- [24] Dante M Kennes, Eli Y Wilner, David R Reichman, and Andrew J Millis. Transient superconductivity from electronic squeezing of optically pumped phonons. *Nature Physics*, 13(5):479–483, 2017.
- [25] M Fechner, M Först, G Orenstein, V Krapivin, AS Disa, M Buzzi, A von Hoegen, G de la Pena, QL Nguyen, R Mankowsky, et al. Quenched lattice fluctuations in optically driven srtio3. *Nature Materials*, pages 1–6, 2024.
- [26] T Boulier, M Bamba, A Amo, Claire Adrados, A Lemaitre, E Galopin, I Sagnes, J Bloch, C Ciuti, E Giacobino, et al. Polariton-generated intensity squeezing in semiconductor micropillars. *Nature communications*, 5(1):3260, 2014.
- [27] Jack Y Qiu, Arne Grimsmo, Kaidong Peng, Bharath Kannan, Benjamin Lienhard, Youngkyu Sung, Philip Krantz, Vladimir Bolkhovsky, Greg Calusine, David Kim, et al. Broadband squeezed microwaves and amplification with a josephson travelling-wave parametric amplifier. *Nature Physics*, pages 1–8, 2023.
- [28] Dan G Cacuci, Mihaela Ionescu-Bujor, and Ionel Michael Navon. *Sensitivity and uncertainty analysis, volume II: applications to large-scale systems*, volume 2. CRC press, 2005.
- [29] Sean Molesky, Zin Lin, Alexander Y Piggott, Weiliang Jin, Jelena Vucković, and Alejandro W Rodriguez. Inverse design in nanophotonics. *Nature Photonics*, 12(11):659–670, 2018.
- [30] Tyler W Hughes, Momchil Minkov, Ian AD Williamson, and Shanhui Fan. Adjoint method and inverse design for nonlinear nanophotonic devices. *AC_s Photonics*, 5(12):4781–4787, 2018.
- [31] Dougal Maclaurin, David Duvenaud, and Ryan P Adams. Autograd: Effortless gradients in numpy. In *ICML 2015 AutoML workshop*, volume 238, 2015.
- [32] Ricky TQ Chen, Yulia Rubanova, Jesse Bettencourt, and David K Duvenaud. Neural ordinary differential equations. *Advances in neural information processing systems*, 31, 2018.
- [33] Joel F Corney, Joel Heersink, Ruifang Dong, Vincent Josse, Peter D Drummond, Gerd Leuchs, and Ulrik L Andersen. Simulations and experiments on polarization squeezing in optical fiber. *Physical Review A*, 78(2):023831, 2008.
- [34] Aruto Hosaka, Taiki Kawamori, and Fumihiko Kannari. Multimode quantum theory of nonlinear propagation in optical fibers. *Physical Review A*, 94(5):053833, 2016.
- [35] S Schmitt, J Ficker, M Wolff, F König, A Sizmann, and Gerd Leuchs. Photon-number squeezed solitons from an asymmetric fiber-optic sagnac interferometer. *Physical review letters*, 81(12):2446, 1998.
- [36] Dmitriy Krylov and Keren Bergman. Amplitude-squeezed solitons from an asymmetric fiber interferometer. *Optics letters*, 23(17):1390–1392, 1998.
- [37] Marlan O Scully and M Suhail Zubairy. Quantum optics, 1999.
- [38] MJ Werner. Quantum soliton generation using an interferometer. *Physical review letters*, 81(19):4132, 1998.
- [39] Andreas Sizmann and Gerd Leuchs. V the optical kerr effect and quantum optics in fibers. *Progress in optics*, 39:373–469, 1999.
- [40] Govind P Agrawal. Nonlinear fiber optics. In *Nonlinear Science at the Dawn of the 21st Century*, pages 195–211. Springer, 2000.
- [41] John M Dudley and James Roy Taylor. *Supercontinuum generation in optical fibers*. Cambridge University Press, 2010.
- [42] PD Drummond and SJ Carter. Quantum-field theory of squeezing in solitons. *JOSA B*, 4(10):1565–1573, 1987.
- [43] Hermann A Haus and Yinchiah Lai. Quantum theory of soliton squeezing: a linearized approach. *JOSA B*, 7(3):386–392,

- 1990.
- [44] Keren Bergman and HA Haus. Squeezing in fibers with optical pulses. *Optics letters*, 16(9):663–665, 1991.
- [45] PD Drummond, RM Shelby, SR Friberg, and Y Yamamoto. Quantum solitons in optical fibres. *Nature*, 365(6444):307–313, 1993.
- [46] SR Friberg, S Machida, MJ Werner, A Levanon, and Takaaki Mukai. Observation of optical soliton photon-number squeezing. *Physical review letters*, 77(18):3775, 1996.
- [47] S Spälter, N Korolkova, F König, A Sizmann, and Gerd Leuchs. Observation of multimode quantum correlations in fiber optical solitons. *Physical review letters*, 81(4):786, 1998.
- [48] Dmitry Levandovsky, Michael Vasilyev, and Prem Kumar. Perturbation theory of quantum solitons:? continuum evolution and optimum squeezing by spectral filtering. *Optics letters*, 24(1):43–45, 1999.
- [49] Kenichi Hiroswa, Hiroto Furumochi, Atsushi Tada, Fumi-hiko Kannari, Masahiro Takeoka, and Masahide Sasaki. Photon number squeezing of ultrabroadband laser pulses generated by microstructure fibers. *Physical review letters*, 94(20):203601, 2005.
- [50] Aruto Hosaka, Masaya Tomita, Tsubasa Otsuka, and Fumi-hiko Kannari. Modal analysis of photon-number statics in a supercontinuum laser pulse. In *European Quantum Electronics Conference*, page EA_10.4. Optica Publishing Group, 2017.
- [51] John M Dudley, Goëry Genty, and Stéphane Coen. Supercontinuum generation in photonic crystal fiber. *Reviews of modern physics*, 78(4):1135, 2006.
- [52] Kristan L Corwin, Nathan R Newbury, John M Dudley, Stéphane Coen, SA Diddams, Karl Weber, and RS Windeler. Fundamental noise limitations to supercontinuum generation in microstructure fiber. *Physical review letters*, 90(11):113904, 2003.
- [53] JN Ames, S Ghosh, RS Windeler, Alex L Gaeta, and Steven T Cundiff. Excess noise generation during spectral broadening in a microstructured fiber. *Applied Physics B*, 77:279–284, 2003.
- [54] Daniel R Solli, Claus Ropers, Prakash Koonath, and Bahram Jalali. Optical rogue waves. *nature*, 450(7172):1054–1057, 2007.
- [55] Shreesha Rao DS, Mikkel Jensen, Lars Grüner-Nielsen, Jesper Toft Olsen, Peter Heiduschka, Björn Kemper, Jürgen Schnekenburger, Martin Glud, Mette Mogensen, Niels Møller Israelsen, et al. Shot-noise limited, supercontinuum-based optical coherence tomography. *Light: Science & Applications*, 10(1):133, 2021.
- [56] Benjamin Wetzel, Alessio Stefani, Laurent Larger, Pierre-Ambroise Lacourt, Jean-Marc Merolla, Thibaut Sylvestre, Alexandre Kudlinski, Arnaud Mussot, Goëry Genty, Frédéric Dias, et al. Real-time full bandwidth measurement of spectral noise in supercontinuum generation. *Scientific reports*, 2(1):882, 2012.
- [57] Thomas Godin, Benjamin Wetzel, Thibaut Sylvestre, Laurent Larger, Alexandre Kudlinski, Arnaud Mussot, A Ben Salem, M Zghal, G Genty, F Dias, et al. Real time noise and wavelength correlations in octave-spanning supercontinuum generation. *Optics Express*, 21(15):18452–18460, 2013.
- [58] Ankit S Disa, Tobia F Nova, and Andrea Cavalleri. Engineering crystal structures with light. *Nature Physics*, 17(10):1087–1092, 2021.
- [59] Alexander von Hoegen, Roman Mankowsky, Michael Fechner, Michael Först, and Andrea Cavalleri. Probing the interatomic potential of solids with strong-field nonlinear phononics. *Nature*, 555(7694):79–82, 2018.
- [60] Michael Kozina, Michael Fechner, Premysl Marsik, Tim van Driel, James M Glownia, Christian Bernhard, Milan Radovic, Diling Zhu, Stefano Bonetti, Urs Staub, et al. Terahertz-driven phonon upconversion in srtio3. *Nature Physics*, 15(4):387–392, 2019.
- [61] Daniele Fausti, RI Tobey, Nicky Dean, Stefan Kaiser, A Dienst, Matthias C Hoffmann, S Pyon, T Takayama, H Takagi, and Andrea Cavalleri. Light-induced superconductivity in a stripe-ordered cuprate. *science*, 331(6014):189–191, 2011.
- [62] Matteo Mitrano, Alice Cantaluppi, Daniele Nicoletti, Stefan Kaiser, A Perucchi, Stefano Lupi, P Di Pietro, Daniele Pontiroli, Mauro Riccò, Stephen R Clark, et al. Possible light-induced superconductivity in k3c60 at high temperature. *Nature*, 530(7591):461–464, 2016.
- [63] TF Nova, AS Disa, Michael Fechner, and Andrea Cavalleri. Metastable ferroelectricity in optically strained srtio3. *Science*, 364(6445):1075–1079, 2019.
- [64] AS Disa, J Curtis, M Fechner, A Liu, A von Hoegen, M Först, TF Nova, P Narang, A Maljuk, AV Boris, et al. Photo-induced high-temperature ferromagnetism in ytio3. *Nature*, 617(7959):73–78, 2023.
- [65] Peter L McMahon, Alireza Marandi, Yoshitaka Haribara, Ryan Hamerly, Carsten Langrock, Shuhei Tamate, Takahiro Inagaki, Hiroki Takesue, Shoko Utsunomiya, Kazuyuki Aihara, et al. A fully programmable 100-spin coherent ising machine with all-to-all connections. *Science*, 354(6312):614–617, 2016.
- [66] Christian Leefmans, Avik Dutt, James Williams, Luqi Yuan, Midya Parto, Franco Nori, Shanhui Fan, and Alireza Marandi. Topological dissipation in a time-multiplexed photonic resonator network. *Nature Physics*, 18(4):442–449, 2022.
- [67] Charles Roques-Carmes, Yannick Salamin, Jamison Sloan, Seou Choi, Gustavo Velez, Ethan Koskas, Nicholas Rivera, Steven E Kooi, John D Joannopoulos, and Marin Soljačić. Biassing the quantum vacuum to control macroscopic probability distributions. *Science*, 381(6654):205–209, 2023.
- [68] Rajveer Nehra, Ryoto Sekine, Luis Ledezma, Qiushi Guo, Robert M Gray, Arkadev Roy, and Alireza Marandi. Few-cycle vacuum squeezing in nanophotonics. *Science*, 377(6612):1333–1337, 2022.
- [69] Melissa A Guidry, Daniil M Lukin, Ki Youl Yang, and Jelena Vučković. Multimode squeezing in soliton crystal micro-combs. *Optica*, 10(6):694–701, 2023.
- [70] Edwin Ng, Ryotatsu Yanagimoto, Marc Jankowski, MM Fejer, and Hideo Mabuchi. Quantum noise dynamics in nonlinear pulse propagation. *arXiv preprint arXiv:2307.05464*, 2023.
- [71] Nicholas Rivera, Jamison Sloan, Yannick Salamin, John D Joannopoulos, and Marin Soljačić. Creating large fock states and massively squeezed states in optics using systems with nonlinear bound states in the continuum. *Proceedings of the National Academy of Sciences*, 120(9):e2219208120, 2023.
- [72] Jamison Sloan, Nicholas Rivera, and Marin Soljačić. Driven-dissipative phases and dynamics in non-markovian nonlinear photonics. *arXiv preprint arXiv:2309.09863*, 2023.
- [73] Yu-Hung Lai, Yu-Kun Lu, Myoung-Gyun Suh, Zhiqian Yuan, and Kerry Vahala. Observation of the exceptional-point-enhanced sagnac effect. *Nature*, 576(7785):65–69, 2019.
- [74] Heming Wang, Yu-Hung Lai, Zhiqian Yuan, Myoung-Gyun Suh, and Kerry Vahala. Petermann-factor sensitivity limit near an exceptional point in a brillouin ring laser gyroscope. *Nature communications*, 11(1):1610, 2020.
- [75] Yaakov Lumer, Yonatan Plotnik, Mikael C Rechtsman, and Mordechai Segev. Self-localized states in photonic topological

- insulators. *Physical review letters*, 111(24):243905, 2013.
- [76] Sebabrata Mukherjee and Mikael C Rechtsman. Observation of floquet solitons in a topological bandgap. *Science*, 368(6493):856–859, 2020.
- [77] Marius Jürgensen, Sebabrata Mukherjee, Christina Jörg, and Mikael C Rechtsman. Quantized fractional thouless pumping of solitons. *Nature Physics*, 19(3):420–426, 2023.
- [78] Martin E Fermann, VI Kruglov, BC Thomsen, John M Dudley, and John D Harvey. Self-similar propagation and amplification of parabolic pulses in optical fibers. *Physical review letters*, 84(26):6010, 2000.
- [79] John M Dudley, Christophe Finot, David J Richardson, and Guy Millot. Self-similarity in ultrafast nonlinear optics. *Nature Physics*, 3(9):597–603, 2007.
- [80] Yoav Lahini, Assaf Avidan, Francesca Pozzi, Marc Sorel, Roberto Morandotti, Demetrios N Christodoulides, and Yaron Silberberg. Anderson localization and nonlinearity in one-dimensional disordered photonic lattices. *Physical Review Letters*, 100(1):013906, 2008.
- [81] Ohad Lib and Yaron Bromberg. Quantum light in complex media and its applications. *Nature Physics*, 18(9):986–993, 2022.
- [82] Logan G Wright, Demetrios N Christodoulides, and Frank W Wise. Controllable spatiotemporal nonlinear effects in multimode fibres. *Nature photonics*, 9(5):306–310, 2015.
- [83] Logan G Wright, Demetrios N Christodoulides, and Frank W Wise. Spatiotemporal mode-locking in multimode fiber lasers. *Science*, 358(6359):94–97, 2017.
- [84] Fan O Wu, Absar U Hassan, and Demetrios N Christodoulides. Thermodynamic theory of highly multimoded nonlinear optical systems. *Nature Photonics*, 13(11):776–782, 2019.
- [85] Logan G Wright, Pavel Sidorenko, Hamed Pourbeyram, Zachary M Ziegler, Andrei Isichenko, Boris A Malomed, Curtis R Menyuk, Demetrios N Christodoulides, and Frank W Wise. Mechanisms of spatiotemporal mode-locking. *Nature Physics*, 16(5):565–570, 2020.
- [86] Logan G Wright, Fan O Wu, Demetrios N Christodoulides, and Frank W Wise. Physics of highly multimode nonlinear optical systems. *Nature Physics*, 18(9):1018–1030, 2022.
- [87] Hamed Pourbeyram, Pavel Sidorenko, Fan O Wu, Nicholas Bender, Logan Wright, Demetrios N Christodoulides, and Frank Wise. Direct observations of thermalization to a rayleigh–jeans distribution in multimode optical fibres. *Nature Physics*, 18(6):685–690, 2022.
- [88] AL Marques Muniz, FO Wu, PS Jung, M Khajavikhan, DN Christodoulides, and U Peschel. Observation of photon-photon thermodynamic processes under negative optical temperature conditions. *Science*, 379(6636):1019–1023, 2023.
- [89] Tobias J Kippenberg, Alexander L Gaeta, Michal Lipson, and Michael L Gorodetsky. Dissipative kerr solitons in optical microresonators. *Science*, 361(6402):eaan8083, 2018.
- [90] Melissa A Guidry, Damiil M Lukin, Ki Youl Yang, Rahul Trivedi, and Jelena Vučović. Quantum optics of soliton microcombs. *Nature Photonics*, 16(1):52–58, 2022.
- [91] Michael Kues, Christian Reimer, Joseph M Lukens, William J Munro, Andrew M Weiner, David J Moss, and Roberto Morandotti. Quantum optical microcombs. *Nature Photonics*, 13(3):170–179, 2019.
- [92] Gal Harari, Miguel A Bandres, Yaakov Lumer, Mikael C Rechtsman, Yi Dong Chong, Mercedeh Khajavikhan, Demetrios N Christodoulides, and Mordechai Segev. Topological insulator laser: theory. *Science*, 359(6381):eaar4003, 2018.
- [93] Miguel A Bandres, Steffen Wittek, Gal Harari, Midya Parto, Jinhan Ren, Mordechai Segev, Demetrios N Christodoulides, and Mercedeh Khajavikhan. Topological insulator laser: Experiments. *Science*, 359(6381):eaar4005, 2018.
- [94] Alexey Gorlach, Ofer Neufeld, Nicholas Rivera, Oren Cohen, and Ido Kaminer. The quantum-optical nature of high harmonic generation. *Nature communications*, 11(1):4598, 2020.
- [95] Maciej Lewenstein, Marcelo F Ciappina, Emilio Pisanty, Javier Rivera-Dean, Philipp Stammer, Th Lamprou, and Paraskevas Tzallas. Generation of optical schrödinger cat states in intense laser–matter interactions. *Nature Physics*, 17(10):1104–1108, 2021.
- [96] Zhuquan Zhang, Frank Y Gao, Yu-Che Chien, Zi-Jie Liu, Jonathan B Curtis, Eric R Sung, Xiaoxuan Ma, Wei Ren, Shixun Cao, Prineha Narang, et al. Terahertz-field-driven magnon upconversion in an antiferromagnet. *Nature Physics*, pages 1–6, 2024.
- [97] Zhuquan Zhang, Frank Y Gao, Jonathan B Curtis, Zi-Jie Liu, Yu-Che Chien, Alexander von Hoegen, Man Tou Wong, Takayuki Kurihara, Tohru Suemoto, Prineha Narang, et al. Terahertz field-induced nonlinear coupling of two magnon modes in an antiferromagnet. *Nature Physics*, pages 1–6, 2024.
- [98] Guillermo Muñoz-Matutano, Andrew Wood, Mattias Johnsson, Xavier Vidal, Ben Q Baragiola, Andreas Reinhard, Aristide Lemaître, Jacqueline Bloch, Alberto Amo, Gilles Nogues, et al. Emergence of quantum correlations from interacting fibre-cavity polaritons. *Nature Materials*, 18(3):213–218, 2019.
- [99] Aymeric Delteil, Thomas Fink, Anne Schade, Sven Höfling, Christian Schneider, and Ataç İmamoğlu. Towards polariton blockade of confined exciton–polaritons. *Nature materials*, 18(3):219–222, 2019.
- [100] Namely, when X follows from a differential equation (such as the nonlinear Schrödinger equation, $(\Delta X)^2$ can be calculated with two differential equation solves, rather than solving over a large ensemble of random initial conditions, solving enough times for acceptable statistical convergence of observables).
- [101] This treatment corresponds to considering the transmission of a light beam with a fixed intensity. This assumption can be realized by a CW input, or a top-hat pulse in a medium with negligible dispersion (as would be for picosecond pulses)
- [102] This approximation while not being particularly rigorous, does track the correct answer well enough to be useful.
- [103] Isolators are used as necessary to avoid back-reflection issues.
- [104] We neglect damping here for simplicity. That said, it can be straightforwardly accommodated in quantum sensitivity analysis (see SI for examples). We consider times below the inverse damping time of this particular phonon (160 fs [59]), which means our conclusions should more or less hold when adding damping.